Magnetocapacitance and loss factor of GaAs quantum Hall effect devices

2014 Metrologia 51 235

(http://iopscience.iop.org/0026-1394/51/3/235)

IOP Publishing | Bureau International des Poids et Mesures Metrologia
Metrologia **51** (2014) 235–242 doi:10.1088/0026-1394/51/3/235

Magnetocapacitance and loss factor of GaAs quantum Hall effect devices

J Schurr, F Ahlers and K Pierz

Physikalisch-Technische Bundesanstalt, 38116 Braunschweig, Germany

Received 6 January 2014, revised 14 March 2014
Accepted for publication 17 March 2014
Published 13 May 2014

Abstract

We present a simple and accurate coaxial bridge capable of measuring the magnetocapacitance and the associated loss factor of a quantum Hall effect device, with and without an external Hall current—a situation where commercial instruments are limited. We interpret the results in terms of the model of compressible and incompressible regions in the two-dimensional electron gas and we deduce a novel empirical relation between the loss factor and the voltage dependence of the magnetocapacitance. This highlights the reason for the linear voltage dependence of the loss factor whose elimination is the basis for all metrological applications of the quantum Hall resistance at alternating current.

Keywords: magnetocapacitance, quantum Hall effect, loss factor

1. Introduction

The integer quantum Hall effect (QHE) denotes the occurrence of plateaux in the Hall resistance according to $R_H = R_K/i$ with the integer number i, and R_K as the von-Klitzing constant, along with the simultaneous vanishing of the longitudinal resistance R_{xx} [1]. The quantum Hall resistance (QHR) is usually applied in resistance metrology at the $i = 2$ plateau.

After the great success in maintaining the dc resistance unit, it was proposed by PTB in 1992 to operate the QHR with alternating current (ac) and to also derive the capacitance unit from this fixed point [2]. The subsequent research discovered curved ac plateaux with a linear frequency and voltage dependence. This was not understood until measurements of the magnetocapacitance of the two-dimensional electron gas (2DEG), and the associated loss factor, explained this as a magnetocapacitive effect [3].

The magnetocapacitance is the capacitance between the 2DEG and a parallel metal electrode, whereby the term 'magneto' refers to the special features of the 2DEG which occur only in a strong magnetic field. In particular, the 2DEG does not behave like a conventional metal electrode because only the compressible regions of the 2DEG shield electric fields similarly to a metal. A magnetocapacitance measurement senses only these regions (as far as they are not isolated from the contacts) and thus can make an important contribution to the understanding of the QHE. A review of the QHE measured with dc and ac can be found, for example, in [4, 5].

The techniques developed to eliminate the capacitive effects from the ac QHR [3, 6–8] all make use of the linear voltage dependence of the loss factor, although the reason for this linearity was not fully understood. We therefore take up this matter and demonstrate the potential of precision measurements of the magnetocapacitance. First, we describe the measurement technique and interpret the features of the magnetocapacitance in terms of the model of compressible and incompressible 2DEG regions. Then, we deduce a novel empirical relation which gives a new insight into the loss factor and its linear voltage dependence.

2. Coaxial capacitance bridge

Coaxial ac bridges [9] were developed at the national metrology institutes for the comparison of decadic impedance standards with a very low relative uncertainty of a few parts in 10^9, at the expense of a high degree of complexity. However, the magnetocapacitance of a QHE device has a small value and the uncertainty requirement is moderate so that a much simpler coaxial bridge is sufficient (figure 1). It is also capable of accurately measuring the loss factor even in the case of long leads into a cryostat—a situation where non-coaxial commercial capacitance bridges usually fail. In contrast to a non-coaxial bridge, the lead corrections are well-defined and very small. The term 'coaxial' is always used here in the sense of an equal and opposite return current in each outer conductor which makes the bridge immune to electrical interference. The resulting low-noise level corresponds to a standard deviation of 5 aF (at 1 pF, a voltage of 100 mV, and an integration time of 30 s).

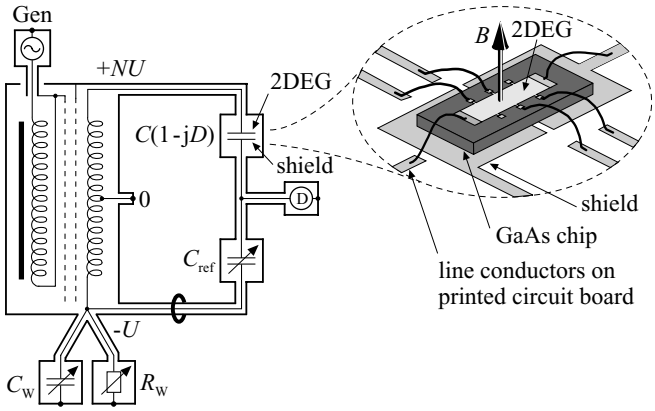

Figure 1. Schematic diagram of a coaxial two-terminal-pair bridge [9] measuring the unknown capacitance C in terms of C_{ref}. The transformer ratio can be set to either 1 : 1, 10 : 1, or 1 : 10. C_W and R_W are Wagner components adjusted to null the current in the zero tap of the ratio transformer.

For our purpose, a two-terminal-pair bridge (as already used in [8, 10]) is sufficient because the capacitance to be measured has a small value and lead corrections are negligible. The schematic representation of such a bridge is shown in figure 1. It measures the unknown capacitance C and the associated loss factor $D = \tan\delta$ in terms of a reference capacitor C_{ref} with a negligible loss factor (in our case less than 1×10^{-5}). Because the capacitances involved have a small value, the bridge transformer is only weakly loaded. Therefore, separate supply and ratio transformers are not needed. Only a Wagner arm to balance the asymmetrical transformer loading might be necessary. An injection system for the bridge balance is also not needed. It is sufficient to roughly balance the reference capacitor and to measure the residual imbalance of the detector voltage. A commercial lock-in amplifier is used as the detector. Its phase is adjusted by a temporary imbalance of the reference capacitor and the unknown loss factor is determined from the quadrature component of the detector voltage.

As a reference capacitor, a low-loss rotary-vane precision parallel-plate capacitor is used. A common type has two ranges, from 50 fF to 1.1 pF and from 500 fF to 11 pF. Taking into account that the bridge transformer can be configured for a 1 : 1, 10 : 1, or 1 : 10 ratio, the total measuring range goes from 5 fF to 110 pF. The reproducibility of the reference capacitor is about 0.5 fF, mainly due to a very small mechanical slip and due to the lack of temperature control, and this determines the uncertainty of the capacitance measurement[1]. The uncertainty of the loss factor is 1×10^{-5} ($k = 1$). To demonstrate the accuracy of the simple coaxial bridge, appendix A shows a measurement of a 1 pF capacitance standard and its associated loss factor in comparison with a commercial capacitance bridge. Appendix A also gives some more information on the uncertainties.

[1] As an alternative to the bridge shown in figure 1, it is also possible to use a fixed-value reference capacitor and to replace the ratio transformer with a decade inductive voltage divider. If a temperature-stabilized fused-silica capacitance standard of either 1 pF, 10 pF or 100 pF would be used as the reference, the limitations of the rotary-vane capacitor could be overcome, if required.

3. QHE devices and potential distribution

The present knowledge of the potential and current distribution in the 2DEG is discussed in [11–16] and briefly summarized here: at the edge of the 2DEG where the electron density drops to zero, the energy levels are bent upwards so that the electrons are confined in the 2DEG. This leads to the formation of compressible and incompressible strips along the edge of the 2DEG. 'Compressible' refers to the ability of the electrons at the Fermi edge to move to other free states. Therefore, the compressible strips are equipotential regions which shield electric fields similarly to a metal and carry no Hall current. In contrast, the incompressible strips are transparent to electric fields like a dielectric, carry a Hall current, and a Hall voltage drop occurs there.

In the bulk of the 2DEG, the disordered potential landscape of the 2DEG is filled with electrons up to the Fermi energy and this creates a landscape of compressible and incompressible regions. In the central plateau region, the bulk of the 2DEG is maximal incompressible with embedded small compressible 'puddles' and carries a fraction of the dissipationless Hall current only in the presence of a close-by gate [18]). Towards the inter-plateau regions, the compressible puddles become much larger, merge into a network with embedded incompressible 'islands', and carry the main part of the now dissipative Hall current, unaffected by the presence of a gate.

All capacitance measurements reported here were carried out at GaAs/AlGaAs devices manufactured at PTB. The charge carrier density is $4.8 \times 10^{15}\ \mathrm{m}^{-2}$ and the dimensions of the 2DEG are 2.6 mm × 0.8 mm. The QHE devices are double-shielded [7] to allow precision measurements of the ac quantum Hall resistance [8]. A double-shielded device is surrounded by two rectangular shields which are arranged in such a way that the narrow gap between them is close to the defining Hall potential contacts. For simplicity, only the dominating bottom part of the shield is shown in figure 1. The magnetocapacitance investigated here is the capacitance between the 2DEG and one half-shield. The geometry is not the very best for a precision measurement of the magnetocapacitance, but we wanted to gain information on our real double-shielded QHE devices. To improve the accuracy, the results have been corrected for the separately measured cross-capacitance between the two half-shields (445 fF) and for the calculated capacitance between the metallic contact pads and the half-shield (104 fF). The loss factor has been corrected for the contribution from the printed circuit board and the GaAs substrate (3.2×10^{-4}). Even though the geometry is complicated, we think that the boundary effects and stray capacitances do not significantly affect the main findings.

Normally, six of eight terminals of a double-shielded QHR device are bonded to allow a so-called triple-series connection scheme [19, 20]. In contrast, a magnetocapacitance measurement requires only one terminal. Indeed, the unneeded terminals cannot be left open-circuited because the lead capacitances C_L would draw considerable currents through the QHE device and the corresponding Hall voltages would appear as an apparent loss factor which is orders of magnitude larger

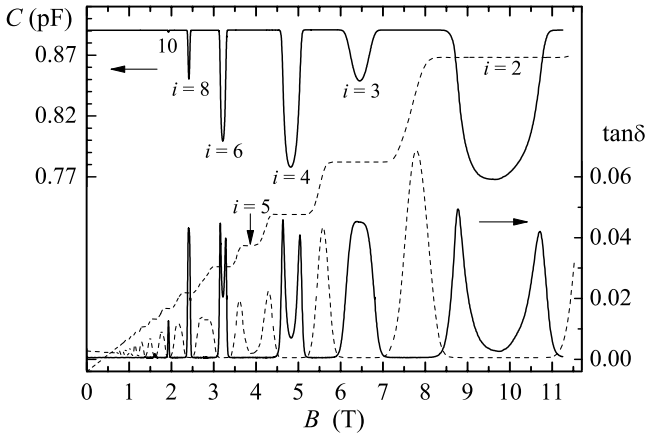

Figure 2. The magnetocapacitance C of a QHE device (top curve with left-hand scale) and the associated loss tangent (right-hand scale), measured as a function of magnetic flux density at a frequency of 1 kHz, a bath temperature of 0.3 K, and an rms voltage of 200 mV. The dashed lines indicate the dc quantum Hall and longitudinal resistance and are given without a scale, just as a guide to the eye.

than the true loss factor of the 2DEG. One possible solution is to use a special QHE device manufactured with only a single terminal (as in [3]). Here we present a new solution which is a modification of the multiple-series connection scheme [19, 20] and can be applied to any multi-terminal QHE device, to allow the full spectrum of characterization measurements at one and the same device. This connection scheme is described in appendix B.

4. Experimental results

Figure 2 shows the magnetocapacitance measured without an applied Hall current. The sweep rate of the superconducting solenoid is set in such a way that the existing structures are not significantly deformed and in particular that no peaks are lost or smeared out. First, we will discuss the magnetocapacitance and then the loss factor.

4.1. Magnetocapacitance

In the inter-plateau regions, the magnetocapacitance is flat and has nearly the same value as at zero magnetic flux density (figure 2). This is attributed to the 2DEG being mainly compressible. In the central plateau regions, the magnetocapacitance exhibits depressions because the bulk of the 2DEG becomes mainly incompressible and transparent to electric fields [12, 16] so that its contribution to the magnetocapacitance is reduced.

This general behaviour is in agreement with former magnetocapacitance measurements [3, 21], only the depressions have different depths. We attribute this to the different spacing between the 2DEG and the gate. In the case of a sub-μm spacing as in [21], the minima of the magnetocapacitance are of the order of one per cent of the geometrical capacitance at zero magnetic field. The reason is that in the central plateau region the magnetocapacitance originates mainly from the compressible edge strips and the electric fields are concentrated in the small space between these edge strips and their projection onto the gate. In our case, the spacing is 450 μm, i.e. much larger than the width of the edge strips. Therefore, the electric fields between the edge strips and the gate are spread over a larger fraction of the space between the 2DEG and the gate. As a result, the relative depth of the depressions is smaller. With a simple stripline model, we estimate the width of the compressible strips at $i = 2$ to be smaller than 1 μm, very similar to [21].

Each depression in figure 2 occurs in a range of magnetic flux density where the longitudinal resistance vanishes and the Hall resistance is accurately quantized. (On a coarse scale, the Hall plateaux seem to be much wider, but this is a misleading impression because the outermost parts of the plateaux do not exhibit an accurate quantization.) At our bath temperature of 0.3 K, the well-defined QHR plateaux with a vanishing longitudinal resistance are the even ones up to $i = 10$ and the odd one $i = 3$ (whereas $i = 1$ is out of the range of our superconducting solenoid). The plateau $i = 5$ is clearly visible in the dc QHR, but it has no central region with a vanishing longitudinal resistance and no accurate quantization. Therefore, it is fully absent in the magnetocapacitance even if the scale is enlarged to the noise limit. This applies even more to the higher odd plateaux and also to the even ones higher than $i = 10$. This clearly shows that the accurately quantized state with a vanishing longitudinal resistance (not to be confound with the wider, only coarsely flat Hall plateau) is strictly tied to the mainly incompressible state of the 2DEG.

Figure 3 shows the magnetocapacitance around $i = 2$ at a higher resolution and measured at different voltages. We distinguish between three regimes with different behaviour which in the following are interpreted in the model of the compressible and incompressible 2DEG regions as developed in [13–16].

In regime III, the Hall resistance is quantized to a high relative degree of at least 1×10^{-9}. In this regime, the magnetocapacitance has a weakly curved shape and a small linear voltage dependence. This is interpreted as follows: the bulk is mainly incompressible with embedded fine-grained compressible puddles. These puddles are isolated from the contacts and thus not cyclically charged. Consequently, only the compressible strips contribute to the magnetocapacitance. Because the incompressible regions do not shield electric fields and contract with increasing electric field strength in favour of the compressible area, the magnetocapacitance increases with the applied voltage.

In regime II, the Hall resistance is still quantized within a relative uncertainty of at least 5×10^{-5}. The compressible puddles in the bulk become larger and constitute a network with embedded coarse-grained incompressible islands. As far as the compressible regions touch the contacts, they are cyclically charged and thus increasingly contribute to the magnetocapacitance. The local electric field in the incompressible regions becomes larger and causes a larger contraction in favour of the compressible regions. As a result, the magnetocapacitance sensing the compressible area exhibits a larger increase with voltage.

Regime I is the inter-plateau region where the longitudinal resistance is already larger than 10 Ω. (The innermost

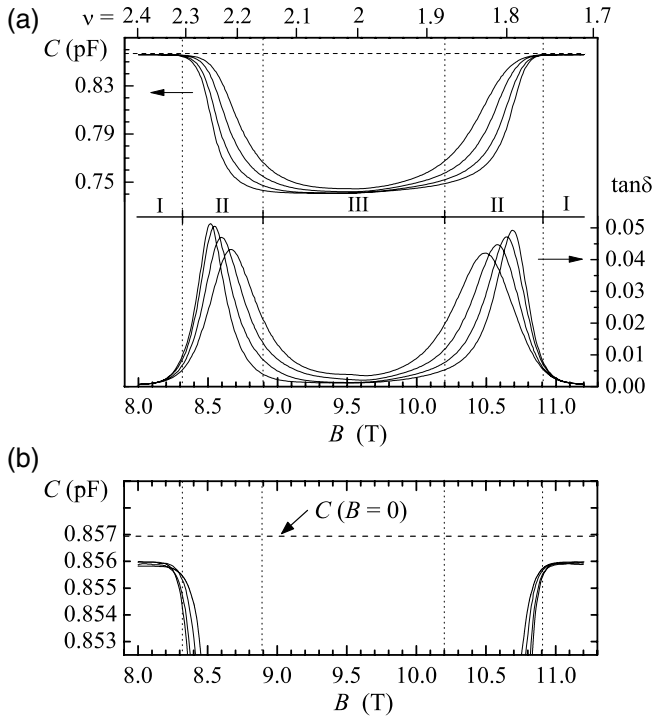

Figure 3. (a) The magnetocapacitance C of a QHE device (left-hand scale) and the associated loss tangent (right-hand scale), measured as a function of magnetic flux density at the $i = 2$ plateau, at a frequency of 1 kHz and a bath temperature of 0.3 K. The rms voltages from top to bottom are 400 mV, 200 mV, 100 mV and 50 mV. The abscissa at the top gives the associated filling factor ν. Three regimes I, II and III are indicated. (b) The same magnetocapacitance data at a higher resolution. The dashed line indicates the capacitance value measured at zero magnetic flux density.

parts of this regime correspond to the outermost parts of the Hall plateau, but even there the Hall resistance is not fully quantized and the plateaux on a finer scale are no longer flat.) In this regime, the magnetocapacitance is flat and voltage-independent. This is interpreted as follows: Coming from regime II, the incompressible islands in the bulk further decrease so that the 2DEG becomes mainly compressible (and dissipative), apart from the incompressible edge strips and some small residual incompressible islands. Thus, the magnetocapacitance approaches a value close to the geometrical capacitance. Because the incompressible regions are now much smaller and fine-structured, the electric field therein is shielded much more effectively. The small incompressible area together with the small electric field therein thus explains the practically vanishing voltage dependence of the magnetocapacitance.

The value of the magnetocapacitance in regime I is smaller than the value obtained at zero magnetic flux density by (1.0 ± 0.1) fF (bottom part of figure 3). This is attributed to the incompressible edge strips which do not exist at zero magnetic flux density. From this, we estimate the width of the incompressible strips at either side of the 2DEG to be about 0.5 µm, in reasonable agreement with other results [21] and very similar to the width of the compressible strips.

The aspects discussed so far are in qualitative agreement with the picture developed in [13–16]. In contrast, our results show a symmetry with respect to the integer filling factor, whereas [13–16] present asymmetric behaviour. We attribute this difference to three facts. Firstly, our QHE devices have much larger dimensions. Secondly, a magnetocapacitance measurement does not sense compressible puddles in the bulk which are isolated from the contacts. And thirdly, our results are obtained without an applied Hall current. Our first results with applied Hall current also show a clear asymmetry, but the details are quite complex and require more research before the results can be published.

Finally, we would like to relate our results to the breakdown of the QHE at large currents [17]. Even if no Hall current is applied, the width of the central depression of the magnetocapacitance decreases with increasing voltage (see figure 3). As a first consequence, the precisely quantized regime III is expected to disappear at a voltage level of a few volts, although the capacitive current is more than four orders of magnitude smaller than the breakdown current. And secondly, in the case of an applied Hall current (well below the breakdown), the voltage-induced contraction of the incompressible regions increases the local current density therein and this could cause a voltage-induced boost of those effects which finally lead to the breakdown. Since we have not investigated this aspect, we will leave it to the future.

4.2. Loss factor

The loss factor of the 2DEG is also shown in figures 2 and 3. At the $i = 2$ plateau, the loss factor shows a peak at either side of the plateau centre. With increasing integer filling factor, these peaks merge together to a single peak which finally disappears. Correspondingly, the width of the vanishing longitudinal resistance and the width of the accurately quantized Hall resistance decreases. Resolving these plateaux, as well as the depression of the magnetocapacitance and the associated loss factor peaks, would require a lower bath temperature (the lower, the larger the integer filling factor). Our ^{3}He system allows only the investigation of the $i = 2$ plateau, but this plateau has the highest relevance to the application of the QHR as an electrical impedance standard. We therefore restrict the analysis to the $i = 2$ plateau.

In the inter-plateau regime I as well as at zero magnetic field, the loss factor of the 2DEG is small (2.3×10^{-4}) and independent of voltage and frequency, similar to conventional dielectric materials at such low temperatures. In the central plateau region III, the loss factor is larger and exhibits a linear voltage dependence (figures 3 and 4). Extrapolating the loss factor in regime III to zero voltage yields the same small value as in the inter-plateau regime I and at zero magnetic flux density. In the transition regions II, the loss factor shows pronounced peaks and a maximum voltage dependence (figures 2 and 3).

Finally, figure 5 shows that the magnetocapacitance as well as the loss factor do not exhibit a significant frequency dependence (at least in the kHz frequency range and within the resolution of our measurement). This was already found in previous works, for example [3, 10], but is shown here with higher accuracy.

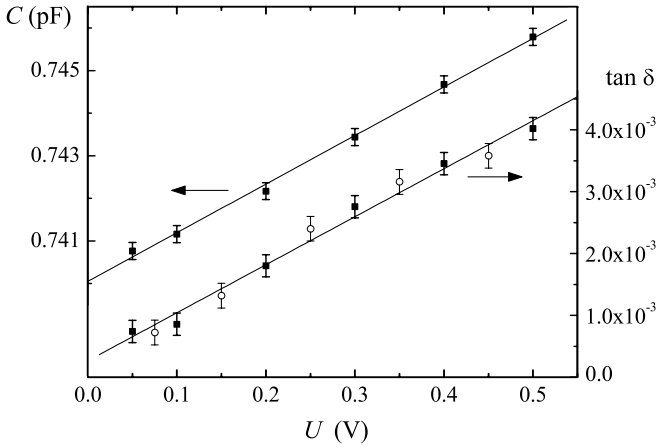

Figure 4. The magnetocapacitance C (left-hand scale) and the associated loss tangent (right-hand scale) at $i = 2$ of the same QHE device as in figure 3, measured as a function of the applied rms voltage U at a frequency of 1 kHz and a bath temperature of 0.3 K. The open symbols are calculated according to (1) with a fitted value $\chi = 0.485$ and with the measured value $\tan\delta_0 = 2.3 \times 10^{-4}$.

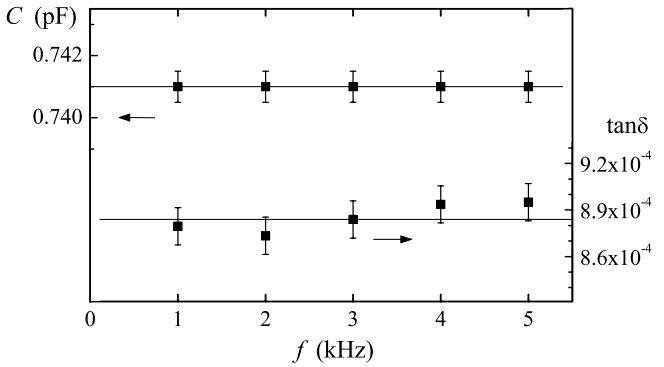

Figure 5. The magnetocapacitance C (left-hand scale) and the associated loss tangent (right-hand scale) of the same QHE device as in figure 4, measured at $i = 2$ as a function of frequency at an rms voltage of 100 mV.

4.3. Model of the loss factor

In [22], the loss factor of the 2DEG has been attributed to polarization losses. This explains the frequency-independence of the loss factor, which for a long time had been an unexplained mystery of the ac QHR [5]. Nevertheless, this model could not explain the observed dependence of the loss factor on magnetic flux density and voltage, and the voltage dependence of the magnetocapacitance was beyond the scope of the model.

Here we would like to add a novel aspect, based on the voltage dependence of the magnetocapacitance. To quantify the increase of the magnetocapacitance C with the rms voltage U, we calculate the derivative $\mathrm{d}C/\mathrm{d}U$, whereby the linearity of the voltage dependence justifies replacing the infinitesimal differences by the measured finite differences. To obtain a dimensionless quantity, we multiply by a normalizing factor U/C and define a quantity $X = U/C \cdot \mathrm{d}C/\mathrm{d}U$ (which is the relative change of capacitance to the relative change of voltage).

As deduced from the measurements of the magnetocapacitance and the dc longitudinal resistance [23–25], the incompressible regions of the 2DEG contract with increasing local

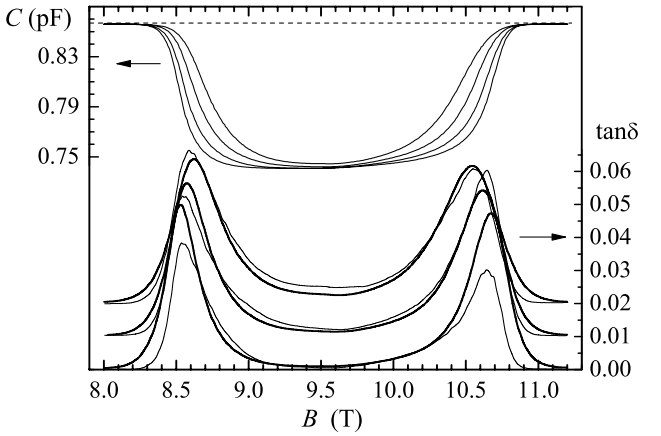

Figure 6. Top: the same magnetocapacitance C as already shown in figure 3. Bottom: from each pair of original loss factor curves measured at two successive voltages, the mean value has been calculated (thick lines) and is compared with the loss factor calculated according to (1) with $\chi = 1$ (thin lines). For better visibility, an arbitrary offset has been added.

electric field strength. This means for the ac case, firstly, that the size of the incompressible regions cyclically alternates, and secondly, that the rms size of the incompressible regions decreases with the rms value of the local electric field. Consequently, the rms value of the compressible area (which is the complement of the incompressible area and sensed by a magnetocapacitance measurement) increases with the rms value of the applied voltage. The quantity X defined above is thus interpreted as a measure of the incompressible fraction of the 2DEG weighted with the local electric field strength.

The contraction of the incompressible regions means a displacement of the localized electrons in the incompressible regions by the local electric field, analogous to the displacement polarization of a dielectric material. We describe this by a quantity χ which is analogous to the imaginary part of the electrical susceptibility, even though we do not have a microscopic model. Taking into account that the polarizing electric fields are only present in the incompressible fraction of the 2DEG, described by the quantity X, the loss tangent of the 2DEG can be written as

$$\tan\delta = \chi \cdot \frac{U}{C} \cdot \frac{\mathrm{d}C}{\mathrm{d}U} + \tan\delta_0, \qquad (1)$$

whereby $\tan\delta_0$ takes into account the polarization losses which occur independent of a magnetic field.

Figure 6 shows the loss factor calculated according to (1) as a function of magnetic flux density in comparison to the measured loss factor. For simplicity, χ has been set to 1. The agreement is remarkably good, though not perfect. It would become even better if χ would vary from about 0.5 at the plateau centre to 1 in regime II. (The remaining deviations might be due to the overly simple model.) Also the voltage dependence of the loss factor calculated according to (1) agrees well with the measured results (see the open symbols in figure 4). In any case, the remarkable finding is that the loss factor stands in a fixed physical relation to the voltage dependence of the magnetocapacitance. The link is

the local electric field which causes both the contraction and the polarization of the incompressible regions.

We would like to emphasize that the ac losses of the incompressible regions are remarkably high, of the order of 1, and this is about four orders of magnitude higher than for conventional dielectrics at the same temperature. However, an incompressible quantum conductor is not a conventional dielectric and, fortunately, the polarising electric fields are quite weak due to the extensive shielding of the embedded compressible regions so that the overall loss factor is not that large.

5. Conclusion

A simple coaxial bridge allows the accurate measurement of the magnetocapacitance and the loss factor of GaAs quantum Hall effect devices. The dependence of the magnetocapacitance on filling factor and voltage is interpreted in terms of compressible and incompressible regions of the 2DEG. In the central plateau region, the capacitive charging current flows mainly through the compressible edge strips, whereas in the inter-plateau regions the charging current is distributed over the whole bulk. Furthermore, the magnetocapacitance is voltage dependent because the incompressible regions contract due to the electric field therein which in turn is responsible for the polarization losses. Therefore, the loss factor stands in a fixed physical relation to the voltage dependence of the magnetocapacitance. This also explains the linear voltage dependence of the loss factor, which has so far not been understood although it is used in all approaches to eliminating the capacitive ac losses from the ac QHR.

In a next step, we will apply the measuring technique also to graphene, a two-dimensional carbon monolayer with unique properties [26], to explore its ac behaviour and to assess its potential as an alternative quantum Hall impedance standard.

Acknowledgments

The authors are grateful to B P Kibble for valuable discussions, to B Hacke and H Marx for manufacturing the QHE devices, and to V Bürkel for providing technical support. The work was performed within EMRP project SIB51. The EMRP is jointly funded by the EMRP participating countries within EURAMET and the European Union.

Appendix A. Comparison with a commercial capacitance bridge and uncertainty contributions

To demonstrate the accuracy of the simple coaxial capacitance bridge used in this work, a parallel-plate capacitor with a nominal value of 1 pF and a low, but significant loss factor has been measured with short leads at room-temperature and compared with a measurement by a commercial, non-coaxial capacitance bridge (figure A1). The results are in good agreement within the particular uncertainty. They also show that the reference capacitor does not exhibit a significant frequency dependence in the frequency range investigated here. The voltage dependence of the reference capacitor has not been explicitly measured, but is typically of the order of $10^{-10}\,\mathrm{V}^{-1}$ and hence negligible for our application.

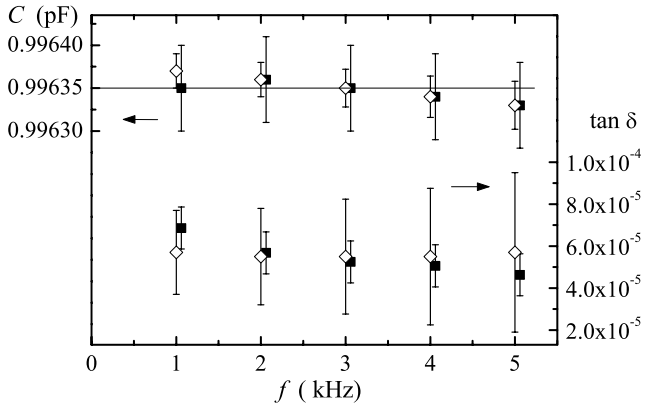

Figure A1. The capacitance C (left-hand scale) and the associated loss tangent (right-hand scale) of a parallel-plate capacitor measured as a function of frequency at an rms voltage of 500 mV. Solid symbols are the results of the simple coaxial bridge and open symbols are the results obtained by a commercial capacitance bridge. For a better visibility, the data of the coaxial bridge have been slightly shifted in frequency. The uncertainty bars correspond to coverage factor $k = 1$.

The bridge transformer can be configured for a 1 : 1, 10 : 1, or 1 : 10 ratio. In each configuration, the transformer ratio usually deviates from nominal. The deviation is typically below 1×10^{-6} and thus negligible here. If required, the 10 : 1 ratio could be calibrated by a separate set-up [9] and the 1 : 1 deviation could be eliminated by a reversal measurement.

The uncertainty of the capacitance measurement is limited by the resolution and repeatability of the rotary-vane reference capacitor. Using a fixed-value reference capacitor and replacing the ratio transformer with a decade inductive voltage divider (as already mentioned in section 2), the relative uncertainty could be reduced to a value as low as 1×10^{-7}.

The loss factor of the reference capacitor is lower than 1×10^{-5} (and also lower than the loss factor uncertainty of the commercial bridge) and this is the main uncertainty contribution to the loss factor of the capacitor under test. The loss factor of the reference capacitor could be determined by other methods with an uncertainty of about 2×10^{-6} [28].

The type A uncertainty of both the capacitance and the loss factor at an integration time of 3 s and an rms voltage of 500 mV amounts to 2×10^{-6} and can be further reduced by a longer integration time or by using a low-noise pre-amplifier (see, for example, the appendix of [29]).

The user has to fix the desired uncertainty and this determines the required effort. In our case, the ultimate uncertainty is not needed so that the bridge can be simple. The main point for our application is that the uncertainty does not significantly increase when a capacitance through long leads into a cryo-magnetic system is measured. This applies in particular to the loss factor whose measurement by a commercial bridge usually fails in that case.

Appendix B. Connection scheme of QHE devices

The QHE devices investigated here are manufactured at PTB for a triple-series connection scheme [19, 20], as shown

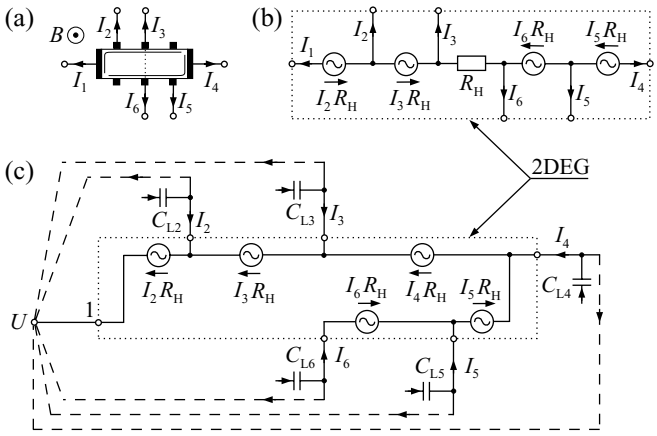

Figure B1. (a) Schematic representation of a QHE device with eight terminals of which two are not bonded. (b) Equivalent circuit [27]. (c) Equivalent circuit of a QHE device at which lead 1 is used for a magnetocapacitance measurement. To avoid that the leads attached to the other terminals remain open-circuited, they can be connected to lead 1 at a star point outside of the cryostat (as indicated by the dashed lines). The Hall resistance element has been omitted because no external Hall current is applied. The lead capacitances C_L are also indicated. For simplicity, the outer conductors are not shown.

in figure B1(a), so that the Hall voltage can be measured orthogonally to the Hall current. The equivalent circuit of such a six-terminal device (figure B1(b) [27]) can be adapted to the situation of a magnetocapacitance measurement whereby only one terminal is connected to the capacitance bridge and no external Hall current is applied (figure B1(c)).

If unused leads connected to the QHE device remain open-circuited, the lead capacitances C_L draw a considerable current through the QHE device. The resulting Hall voltages appear as an apparent contribution $\omega R_H C_L$ to the loss factor which in our case amounts to $3.5 \times 10^{-2}\,\mathrm{kHz}^{-1}$, independent of whether the 2DEG is connected to the high- or to the low-potential side of the capacitance bridge. This unwanted effect would completely cover the loss factor of the 2DEG.

Our new solution is a modification of the multiple-series connection scheme [19, 20]: all leads attached to the QHE device have to be connected to a single star point (as shown in figure B1(c) which in turn is connected to the capacitance bridge. The lead capacitive currents now flow off along the leads, but they no longer flow through the QHE device. The lead capacitances asymmetrically load the bridge transformer, but this can be compensated for by the Wagner arm. Because the leads have a certain lead resistance R_L, a corresponding voltage drop occurs at each lead. The multiple-series connection compensates for this except for the usual two-terminal-pair lead contribution to the loss factor, $\omega R_L C_L/2$. This contribution is very small (5×10^{-6} at a frequency of 1 kHz), well-defined and could be corrected for, if desired.

The original multiple-series connection scheme with two star points, as shown in figure B2, can be used to measure the magnetocapacitance of a QHE device through which an external alternating Hall current flows. One star point is to be connected to the high-terminal of the capacitance bridge, whereas the other star point is connected to zero potential (i.e. the outer conductor network). The ac voltage U charging the

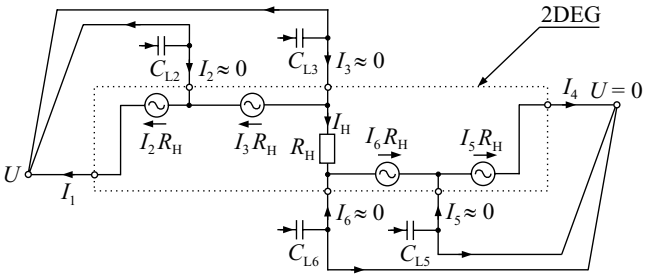

Figure B2. Equivalent circuit of a QHE device for a magnetocapacitance measurement with applied ac Hall current.

magnetocapacitance and the ac voltage driving the Hall current $I_H = U/R_H$ are thus the same, which is exactly the situation of a real ac QHR measurement. Note that the Hall current which is four orders of magnitude larger than the capacitive current does not flow through the reference capacitor; the Hall resistance only appears to the bridge transformer as a weak asymmetrical load which can be compensated for by a Wagner arm, if required.

It is also possible to measure the magnetocapacitance in the presence of a direct Hall current whose magnitude can be set independently of the ac measuring voltage. We suggest to create the direct current by an adjustable battery because a controlled dc current source may cause interference. In any case, the particular transformer must be protected with a large-value blocking capacitor to prevent it from getting strongly magnetised by a dc current.

Finally, we would like to mention that the equivalent circuit does not take a non-zero longitudinal resistance into account. In the case without an applied Hall current, the longitudinal voltage is zero because the Hall current is zero. In the case with an applied Hall current, we measured only under the condition of a small longitudinal resistance where the Hall resistance is at least roughly quantized. The multiple-series connection then compensates for the small longitudinal resistance in the same way as it does at a usual ac QHR measurement.

References

[1] von Klitzing K, Dorda G and Pepper M 1980 New method for high-accuracy determination of the fine structure constant based on quantized Hall resistance *Phys. Rev. Lett.* **45** 494–7

[2] Melcher J, Warnecke P and Hanke R 1993 Comparison of precision ac and dc measurements with the quantized Hall resistance *IEEE Trans. Instrum. Meas.* **42** 292–4

[3] Delahaye F, Kibble B P and Zarka A 2000 Controlling ac losses in quantum Hall effect devices *Metrologia* **37** 659–70

[4] Jeckelmann B and Jeanneret B 2001 The quantum Hall effect as an electrical resistance standard *Rep. Prog. Phys.* **64** 1603–56

[5] Schurr J, Ahlers F and Kibble B P 2012 The ac quantum Hall resistance as an electrical impedance standard and its role in the SI *Meas. Sci. Technol.* **23** 124009

[6] Overney F, Jeanneret B, Jeckelmann B, Wood B M and Schurr J 2006 The quantized Hall resistance: towards a primary standard of impedance *Metrologia* **43** 409–13

[7] Kibble B P and Schurr J 2008 A novel double-shielding technique for ac quantum Hall measurement *Metrologia* **45** L25–7

[8] Schurr J, Kučera J, Pierz K and Kibble B P 2011 The quantum Hall impedance standard *Metrologia* **48** 47–57
[9] Awan S, Kibble B P and Schurr J 2011 *Coaxial Electrical Circuits for Interference-Free Measurements* (London: The IET)
[10] Schurr J, Kibble B P, Hein G and Pierz K 2009 Controlling losses with gates and shields to perfect a quantum Hall impedance standard *IEEE Trans. Instrum. Meas.* **58** 973–9
[11] Chklovskii D B, Shklovskii B I and Glazman L I 1992 Electrostatics of edge channels *Phys. Rev.* B **46** 4026–34
[12] Yacoby A, Hess H F, Fulton T A, Pfeiffer L N and West K W 1999 Electrical imaging of the quantum Hall state *Solid State Commun.* **111** 1–13
[13] Weis J and von Klitzing K 2011 Metrology and microscopic picture of the integer quantum Hall effect *Phil. Trans. R. Soc.* A **369** 3954–74
[14] Ahlswede E, Weitz P, Weis J, von Klitzing K and Eberl K 2001 Hall potential profiles in the quantum Hall regime measured by a scanning force microscope *Physica* B **298** 562–6
[15] Ahlswede E, Weis J, von Klitzing K and Eberl K 2002 Hall potential distribution in the quantum Hall regime in the vicinity of a potential probe contact *Physica* E **12** 165–8
[16] Ahlswede E 2002 Potential- und Stromverteilung beim Quanten-Hall-Effekt bestimmt mittels Rasterkraftmikroskopie *Thesis* Max Planck Institute for Solid State Research, Stuttgart, Germany
[17] Nachtwei G 1999 Breakdown of the quantum Hall effect *Physica* E **4** 79–101
[18] Yahel E, Tsukernik A, Palevski A and Shtrikman H 1998 Evidence for bulk current in Hall bar samples and potential screening in the integer quantum Hall effect *Phys. Rev. Lett.* **81** 5201–4
[19] Delahaye F 1993 Series and parallel connection of multiterminal quantum Hall-effect devices *J. Appl. Phys.* **73** 7914–20
[20] Delahaye F 1995 Accurate ac measurements of the quantized Hall resistance from 1 Hz to 1.6 kHz *Metrologia* **31** 367–73
[21] Takaoka S, Oto K, Kurimoto H, Murase K, Gamo K and Nishi S 1994 Magnetocapacitance and the edge state of a two-dimensional electron system in the quantum Hall regime *Phys. Rev. Lett.* **72** 3080–3
[22] Jeanneret B and Overney F 2007 Phenomenological model for the frequency-related dissipation in the quantized Hall resistance *IEEE Trans. Instrum. Meas.* **56** 431–4
[23] Haug R J, von Klitzing K and Ploog K 1987 Analysis of the asymmetry in Shubnikov–de Haas oscillations of two-dimensional systems *Phys. Rev.* B **35** 5933–5
[24] Svoboda P, Streda P, Nachtwei G, Jaeger A, Cukr M and Láznicka M 1992 Current-induced coupling of the edge and bulk channels in GaAs/Al_xGa_{1-x}As heterostructures *Phys. Rev.* B **45** 8763–6
[25] Nachtwei G, Breitlow C, Seyfarth J, Heide S, Bliek L, Ahlers F-J, Svoboda P and Cukr M 1994 Transition from non-local to local electron conduction at GaAs/GaAlAs heterojunctions *Semicond. Sci. Technol.* **9** 10–6
[26] Geim A K and Novoselov K S 2007 The rise of graphene *Nature Material* **6** 183–91
[27] Schurr J, Ahlers F, Hein G, Melcher J, Pierz K, Overney F and Wood B M 2006 AC longitudinal and contact resistance measurements of quantum Hall devices *Metrologia* **43** 163–73
[28] Ramm G and Moser H 2001 From the calculable ac resistor to capacitor dissipation factor determination on the basis of time constants *IEEE Trans. Instrum. Meas.* **50** 286–9
[29] Schurr J, Moser H, Pierz K, Ramm G and Kibble B P 2011 Johnson–Nyquist noise of the quantized Hall resistance *IEEE Trans. Instrum. Meas.* **60** 2280–5